

## Article

# Doxycycline Removal by Solar Photo-Fenton on a Pilot-Scale Composite Parabolic Collector (CPC) Reactor

Faiza Bensaïbi <sup>1,\*</sup> , Malika Chabani <sup>1</sup> , Souad Bouafia <sup>1</sup> and Hayet Djelal <sup>2,\*</sup> 

<sup>1</sup> Laboratoire Génie de la Réaction, Faculté de Génie des Procédés et Génie Mécanique, Université des Sciences et de la Technologie Houari Boumediene (USTHB), BP 32, El Allia, Algiers 16111, Algeria; mchabani@usthb.dz (M.C.); sc.bouafia@gmail.com (S.B.)

<sup>2</sup> Unilasalle Ecole des Métiers de l'Environnement, Cyclann, Campus de Ker Lann, 35170 Bruz, France

\* Correspondence: fbensaibi@usthb.dz (F.B.); hayet.djelal@unilasalle.fr (H.D.)

**Abstract:** In this study, the solar photo-Fenton (SPF) process was investigated for the degradation of doxycycline (DOX) using a solar compound parabolic collector (CPC) reactor and a borosilicate serpentine tube with an irradiated volume of 1.8 L. The influence of the operating parameters, such as H<sub>2</sub>O<sub>2</sub>, Fe<sup>2+</sup> dosage, and DOX concentration, was investigated. The optimum H<sub>2</sub>O<sub>2</sub>, Fe<sup>2+</sup> dosage, and DOX concentration were found to be 4, 0.1, and 0.06 mM, respectively. The results of photo-Fenton experiments fitted the pseudo-first-order kinetic equation (R<sup>2</sup> = 0.99). The efficiency of the treatment under optimized conditions was analyzed by an HPLC analysis of the samples, chemical oxygen demand (COD), and total organic carbon (TOC). The results obtained showed that the solar photo-Fenton process achieved a DOX degradation of 95.07%, a COD elimination of 81.43%, and a TOC elimination of 73.05%. The phytotoxicity tests revealed a 73.32% decrease in the germination index of watercress seeds, demonstrating that the SPF process minimizes the toxicity of the chemical and did not have any negative impact on plant growth. Overall, the results of this study suggest that SPF is a promising technology for the removal of doxycycline from wastewater.

**Keywords:** solar photo-Fenton process; doxycycline; CPC reactor; wastewater treatment; germination index



**Citation:** Bensaïbi, F.; Chabani, M.; Bouafia, S.; Djelal, H. Doxycycline Removal by Solar Photo-Fenton on a Pilot-Scale Composite Parabolic Collector (CPC) Reactor. *Processes* **2023**, *11*, 2363. <https://doi.org/10.3390/pr11082363>

Academic Editor: Andrea Petrella

Received: 29 June 2023

Revised: 28 July 2023

Accepted: 3 August 2023

Published: 5 August 2023



**Copyright:** © 2023 by the authors. Licensee MDPI, Basel, Switzerland. This article is an open access article distributed under the terms and conditions of the Creative Commons Attribution (CC BY) license (<https://creativecommons.org/licenses/by/4.0/>).

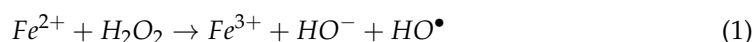
## 1. Introduction

Antibiotics' complex molecular structures can either kill or prevent the growth of bacteria, making exposure to them a possible concern for humans as well as animals [1]. Additionally, their improper or excessive use might induce bacterial resistance and associated antibiotic-resistance genes, which have been labeled as “new emerging environmental contaminants” [2,3]. Doxycycline is a semi-synthetic tetracycline antibiotic that is effective against a wide range of bacteria, including gram-negative, gram-positive, and “atypical” strains as well as protozoa such as malaria. It is used all over the world to treat a variety of infections, including sexually transmitted diseases, respiratory infections, malaria prophylaxis, and rickettsia diseases [4]. The tetracycline antibiotics family is also commonly used to stimulate growth in agriculture and aquaculture. Due to its extensive usage and high stability, it can also disrupt the balance of aquatic species, which results in dysbiosis, and has several adverse consequences on them [5].

Conventional wastewater treatment processes cannot completely degrade pharmaceutical compounds in aquatic ecosystems [6]. Numerous studies have shown the presence of residual DOX in a variety of environmental media, including animal tissues [7] wastewater treatment plants, recycled water, groundwater, streams, and sediments. The excrement from various animal species includes 70% of DOX in the form of prototypes or metabolites [8], which allows DOX to enter surface and groundwater. Additionally, DOX has been found in surface water in Hong Kong at an average value of 0.027 g/L [9] and in river water in China at an average concentration of 0.047 g/L [10]. Maximum DOX concentrations

were detected in Australia at 0.2 g/L in hospital effluent, 0.15 g/L in effluent from sewage plants, and 0.4 g/L in surface water [11]. The ecological environment, the security of agricultural products, and, ultimately, human health are seriously threatened, especially when fertilizers of animal origin are used excessively and are not treated harmlessly, allowing DOX to make its way into the soil and groundwater [12]. Therefore, creating treatment systems for monitoring and removing pharmaceutical compounds, particularly unwanted antibiotic compounds released into the ecosystem, has piqued the attention of researchers and become an increasingly prevalent subject in wastewater treatment [13].

One promising approach is the use of advanced oxidation processes (AOPs), which are based on the production of hydroxyl radicals, as a strong oxidizing agents, to degrade organic pollutants, namely, ozonation [14], photocatalysis [15], electro-Fenton oxidation [16], and Fenton and photo-Fenton oxidation [17]. Among these processes, the photo-Fenton process has gained a lot of attention as an alternative for degrading recalcitrant pollutants due to its high efficiency, operational easiness, and potential to be powered by solar radiation [3]. Solar light accelerates the Fenton reaction by promoting the regeneration of the ferrous ion  $Fe^{2+}$  through the photoreduction of the ferric ion  $Fe^{3+}$  and the creation of extra  $HO^\bullet$  radicals [18]. The photo-Fenton process is an ecologically beneficial application since it uses iron as a catalyst, which is both non-toxic and abundant. Furthermore, the cost of  $H_2O_2$  is lower than that of other oxidants [19]. The reaction between  $Fe(II)$  and  $H_2O_2$  leads to the production of hydroxyl radicals, as shown in Equation (1). The  $Fe(III)$  generated in the first stage then produces ferric aquo complexes ( $[Fe(OH)]^{2+}$ ) as shown in Equation (2). These complexes absorb in a wide range (between 290 and 410 nm). This latter may be reduced in aqueous media by UV light, releasing additional hydroxyl radicals, as shown in Equation (3), and turning the system into a photocatalytic process [20].



Numerous studies have shown the remarkable efficiency of the photo-Fenton process, such as the study of Han et al. [21], which shows that 97.1% of tetracycline and oxytetracycline were removed by the photo-Fenton process ( $UV/H_2O_2/Fe^{2+}$ ) with 20 mg/L of  $H_2O_2$  and 10 mg/L of  $Fe^{2+}$  after 60 min. The photo-Fenton process was more effective than  $H_2O_2$ , ultraviolet (UV), and ( $UV/H_2O_2$ ) at the same doses of oxidants. Another study by Zhong et al. [22] degraded more than 99% of sulfamethoxazole (SMZ), ofloxacin (OFX), and amoxicillin (AMX) after 30 min using the photo-Fenton process. The main disadvantages of the photo-Fenton process are the complexity of design and layout, the high costs of UV reactors, the short operational life cycles of artificial UV sources, and the high energy consumption [23]. These limitations can be overcome by using sunlight that falls on the earth's surface with a wavelength between 290 nm and 800 nm. This radiation can promote direct transformations of organic molecules (direct photolysis) and indirect transformations that occur throughout the interaction of pollutants with photogenerated species [24].

Solar technology has recently evolved the photo-Fenton process into a low-cost and competitive process for removing organic pollutants. This has been confirmed by life cycle assessment (LCA) and integrated environmental-economic index (EEI) studies [25]. The main factors that influence the cost of photo-Fenton treatment are radiation energy and Fenton reagents [26]. One method proposed to reduce the cost associated with photo-Fenton is to use solar radiation, which is a renewable and abundant resource. This can significantly reduce the cost of the treatment, compared to systems that use artificial light sources, particularly at larger treatment scales. Combining this with a pre-treatment or polishing treatment can further reduce the cost. The use of solar reactors is an intriguing alternative for wastewater treatment, with certain advantages. These include the reduction in expenses related to the installation and maintenance of UV lamps and electrical power

consumption [27]. Compared to other designs of solar reactors that only receive direct solar radiation, the CPC reactor is more efficient since all sunlight that reaches the CPC reactor area (direct, diffuse, and reflected radiations) may be collected and delivered to the reactor [28].

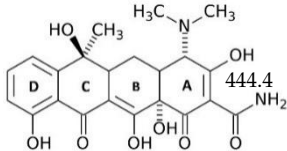
The present study was designed to investigate the efficiency of the degradation of doxycycline by the solar photo-Fenton process on a pilot-scale helio-photochemical reactor (CPC reactor) designed in our laboratory at the USTHB University of Algiers. The reactor is capable of capturing direct, reflected, and diffused sunlight even on cloudy days. Using solar radiation sources as an alternative to conventional lamps reduces the cost of the photo-Fenton process. It's been hypothesized that this approach would be efficient and enable the organic matter to be removed economically, helping to reduce the overall cost of the process as well as reduce the chemical oxygen demand (COD) and the total organic carbon (TOC) of DOX. The analysis focused on the influence of operating parameters on the process. In addition, the study investigated the mineralization of DOX by measuring the chemical oxygen demand (COD) and total organic carbon (TOC). Eventually, the toxicity of the treated effluent was investigated by the phytotoxicity test.

## 2. Material and Methods

### 2.1. Reagents and Chemicals

Doxycycline (C<sub>22</sub>H<sub>24</sub>N<sub>2</sub>O<sub>8</sub>, 99% purity) was obtained from the Algerian pharmaceutical group SAIDAL\_Algeria. The chemical structure and characteristics of DOX are depicted in Table 1.

**Table 1.** Chemical structure and the characteristics of DOX [29].

Scientific Nomenclature	Molecular Formula	Molecular Structure	Molecular Weight (g·mol <sup>-1</sup> )	$\lambda_{max}(nm)$	pKa
Doxycycline	C <sub>22</sub> H <sub>24</sub> N <sub>2</sub> O <sub>8</sub>		444.4	$\lambda_{max1} = 278$ $\lambda_{max2} = 350$	pKa1 = 3.50 pKa2 = 7.07 pKa3 = 9.13

Iron (II) sulfate heptahydrate (FeSO<sub>4</sub>·7H<sub>2</sub>O), with a purity of 98.5%, was purchased from LabKem, France, and hydrogen peroxide 35% (w/v) was purchased from Lab Online, France. The pH was adjusted using sulfuric acid 9N with a purity of 96%, which was purchased from PanReac AppliChem, France. All the solutions were prepared using osmosed water (Milli-Q<sup>®</sup> IX 7003, Merck, Germany).

### 2.2. Experimental Set-Up CPC Reactor

The photo-Fenton tests were conducted at the University of Sciences and Technologies Houari Boumedienne Beb Ezzouer-Algiers (latitude 36.7 N, longitude 3.18 W) in a composite parabolic collector (CPC) photoreactor. This equipment is positioned on a 37° inclination platform, fixed on an aluminum frame (60 cm/60 cm) with aluminum reflectors, with an irradiation area of 376,248 mm<sup>2</sup> and an irradiated volume of 1.8 L.

The serpentine reactor is made up of four borosilicate tubes with a total length of 2900 mm. A centrifugal pump (HALM, Germany) with a flow rate of 30.6 L/min returns the fluid to the concentrators. Figure 1 depicts the photoreactor's properties and dimensions. All experiments in the CPC pilot plant used a 4 L DOX solution delivered to the CPC's unit recirculation tank and homogenized by turbulent recirculation. A pH correction of 3 was performed using sulfuric acid H<sub>2</sub>SO<sub>4</sub> (9N). Before each experiment, the DOX-Fe SO<sub>4</sub> solution was made in the laboratory by dissolving FeSO<sub>4</sub>·7H<sub>2</sub>O in water at pH 3, adding DOX, and homogenizing. The final product was then placed in a tank that was covered to keep the light out. To ensure a homogenous sample and avoid back-mixing, the fluid in the

reactor was kept flowing for approximately three minutes. A preliminary sample was used to determine the correct DOX concentration needed for the operation. Then,  $H_2O_2$  was added to the mixture with a concentration that corresponded to the equation's theoretical stoichiometric value, as shown in Equation (4).

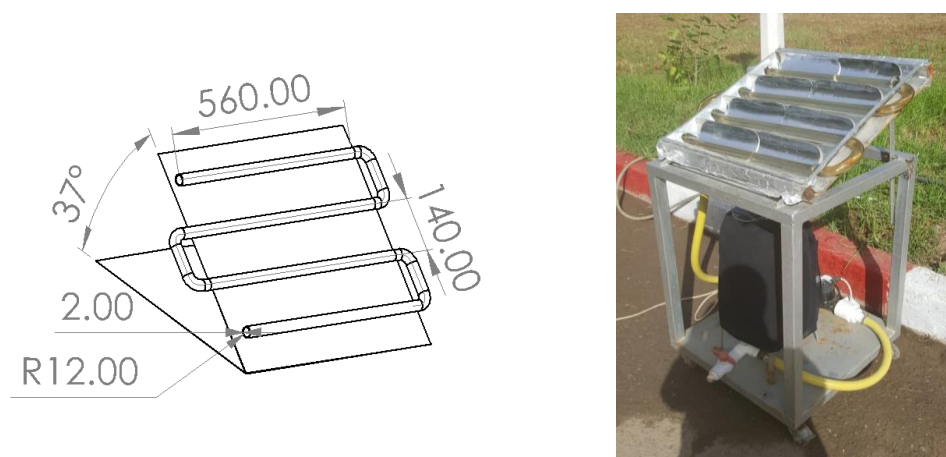
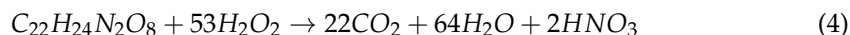


**Figure 1.** Characteristics and dimensions of the CPC reactor.

After that, samples were obtained at various predetermined intervals to evaluate the progress of the oxidation process. The calibration curves at the two maximum wavelengths were plotted by establishing 10 points from 0 to 100 mg/L of DOX concentration and measuring the absorbance of each concentration at the two  $\lambda_{max}$ . Equations (5) and (6) of the calibration curve at 278 and 350 nm, respectively, were used to calculate the concentrations of DOX. The removal efficiency of DOX was determined using Equation (7).

$$y = 0.0288x \quad (R^2 = 0.9992) \quad (5)$$

$$y = 0.0242x \quad (R^2 = 0.9992) \quad (6)$$

$$DOX_{removal}(\%) = \frac{C_0 - C}{C_0} \times 100 \quad (7)$$

### 2.3. Analytical Procedures

The samples were analyzed using a UV/Vis spectrophotometer (P9 Double Beam Spectrophotometer UV/Visible, VWR®, France). pH was measured using a pH meter (pH 3110, pH electrode SenTix®21, Grosseron, WTW, France).

The COD (Spectroquant TR 420, Merck, Frankfurt, Germany) instrument was used to measure COD. The digestion was set for 120 min at 150 °C. The ranges used for COD analysis are 10–150 (mg/L) and 4–40 (mg/L) before and after treatment analysis, respectively. The total organic carbon (TOC) was measured by a (TOC-L Total Organic Analyzer, Shimadzu, France). The COD and TOC experiments were conducted three times, and average values are reported.

DOX concentration (20  $\mu$ L of the sample was injected) was determined using a high-performance liquid chromatograph equipped with a photodiode array detector (Waters 2998, France) and a binary HPLC pump (Waters 1525, France). The data were recorded by EMPOWER 3 software. The stationary phase was a C18 column (3.5  $\mu$ m, 4.6  $\times$  75.0 mm) (Symmetry®, Waters, France), and the mobile was made up of a mix of acetonitrile HPLC grade (20%) and ultra-pure water (80%) which was adjusted to pH 2.5 with concentrated orthophosphoric acid 85 (%) [30] in isocratic flow (0.1 mL·min<sup>-1</sup>). The column was at room temperature (25 °C) and the retention time was 3.46 min. The wavelength of the UV

detector was set at 278 nm and 350 nm. The calibration curve was prepared with different doxycycline concentrations in the range of 1–100 mg/L. MILLIPORE (Synergy®UV, Merck, Germany) was used to prepare the mobile phase and diluent solutions.

#### 2.4. Phytotoxicity Assay

For germination testing, 5 mL of the DOX solution before and after treatment was poured into Petri dishes (Ø 10 cm) lined with filter paper, and 10 Alenois cress seeds from a farm in Saint Marthe, France were inserted equidistantly. Under the same conditions, distilled water served as a control. All Petri plates were placed in an incubator at 25 °C for two days, protected from light. The number of germinated seeds and root length were measured after 48 h [31,32]. The results were analyzed by calculating the index of germination, where the number of germinated seeds, germination rate (%), and root length (mm), were determined by the following equation:

$$GI(\%) = \frac{\text{Seeds germination}(\%) \times \text{Root length of treatment}}{\text{Seeds germination}(\%) \times \text{Root length of control}} \times 100 \quad (8)$$

### 3. Results and Discussion

#### 3.1. Influence of the Operating Parameters

##### 3.1.1. Effect of Iron Dosage Fe<sup>2+</sup>

The efficacy of the photo-Fenton process is negatively impacted by increasing the Fe<sup>2+</sup> content from 0.1 mM to 0.3 mM (Figure 2). Keeping the concentration of H<sub>2</sub>O<sub>2</sub> constant at 4 mM allowed the monitoring of the effect of iron concentration on DOX degradation. At an iron concentration of 0.3 mM, a low DOX degradation rate of 28% was found. Half of the quantity of DOX was eliminated when the iron concentration was lowered to 0.2 mM after 180 min of irradiation (Table 1). The rate of degradation rose considerably when the Fe<sup>2+</sup> concentration was reduced to 0.1 mM. This might be owing to the reduced inhibitory impact of Fe<sup>2+</sup> as its concentration decreases or to reduced turbidity caused by the production of iron sludge at high Fe<sup>2+</sup> levels, which impedes the transmissivity of UV light essential for photodegradation [33,34].

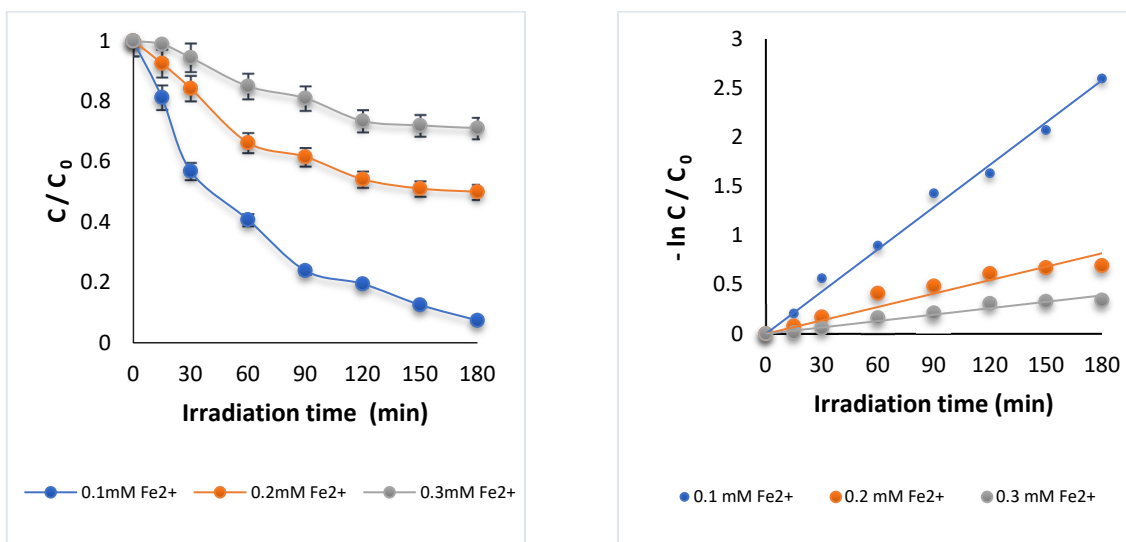


**Figure 2.** Effect of initial [Fe<sup>2+</sup>] on DOX elimination via the solar photo-Fenton process. [DOX] = 0.06 mM, [H<sub>2</sub>O<sub>2</sub>] = 4 mM, pH = 3.

These findings are consistent with the classic Fenton reaction, in which excess Fe<sup>2+</sup> ions serve as hydroxyl radical scavengers, as shown in Equation (9). It is possible that the

speed of the subsequent reaction, which was competitive in the case of high iron amounts, has slowed down, which has an effect on the efficiency of degradation [35,36].



The correlation coefficients ( $R^2$ ) and the percent of degradation (DOX removal (%)) are summarized in Table 2 below. The degradation profile was closely matched with pseudo-first-order kinetics. The kinetic constant rate  $K$  ( $\text{min}^{-1}$ ) was determined from the slope of the linear plot of Equation (10), where  $C_t$  is the concentration at moment  $t$  and  $C_0$  is the starting concentration. The highest value of  $K$  ( $0.0143 \text{ min}^{-1}$ ), close to the  $K$  in the degradation of tetracycline by SPF in the pilot photoreactor [37], corresponded to  $0.1 \text{ mM Fe}^{2+}$  with an  $R^2$  value of 0.99.

$$K * t = -\text{Ln} \left( \frac{C_t}{C_0} \right) \quad (10)$$

**Table 2.** Kinetic parameters, correlation coefficients ( $R^2$ ), and % DOX removal via the solar photo-Fenton process.

$Fe^{2+}$ (mM)	$K$ ( $\text{min}^{-1}$ )	$R^2$	DOX Removal (%)
0.1	0.0143	0.99	92.5
0.2	0.0045	0.91	50.0
0.3	0.0022	0.95	28.0

### 3.1.2. Effect of Initial Concentration of Hydrogen Peroxide Oxidant

The degradation of DOX during the solar photo-Fenton oxidation process was examined under various oxidant concentrations (3 mM, 4 mM, and 5 mM) at pH 3.0 and at a constant ferrous concentration of 0.1 mM in order to determine the optimum  $H_2O_2$  dose. As shown in Figure 3, by increasing the concentration of  $H_2O_2$  from 3 mM to 5 mM, a significant change in the degradation of DOX was observed, yielding a degradation of 51% after 180 min of solar oxidation with 3 mM of  $H_2O_2$  and a degradation of 90% of DOX during the same amount of time of solar photo-Fenton treatment at 4 mM  $H_2O_2$ . However, a further increase of the oxidant dose to 5 mM of  $H_2O_2$  caused a decrease in the DOX degradation rate, as shown in Figure 3.

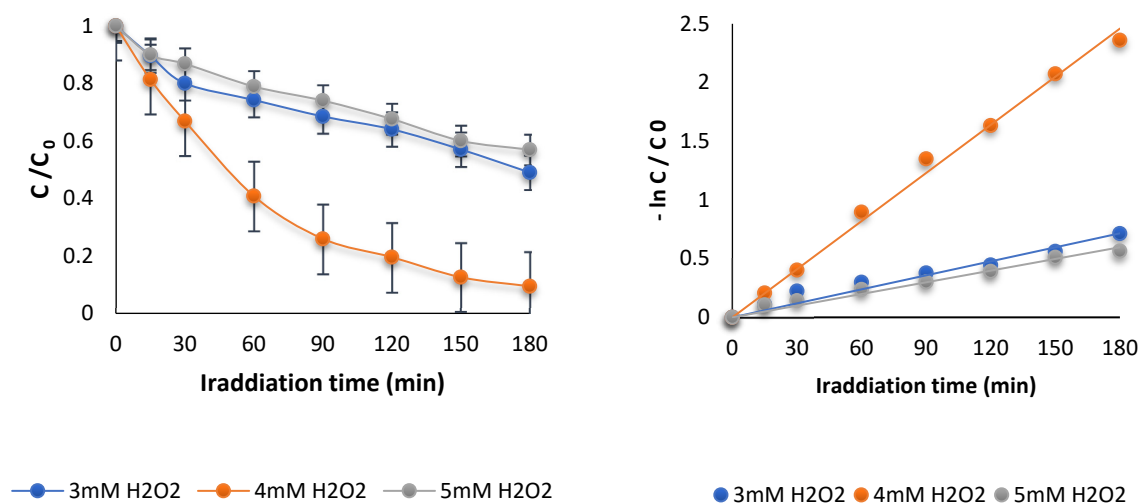


**Figure 3.** Effect of initial  $[H_2O_2]$  on DOX elimination via the solar photo-Fenton process.  $[DOX] = 0.06 \text{ mM}$ ,  $[Fe^{2+}] = 0.1 \text{ mM}$ ,  $\text{pH} = 3$ .

The progressive increase in  $H_2O_2$  concentration allows for the generation of more hydroxyl radicals, which are required for the oxidation of DOX. This can have an adverse

effect because the excess hydrogen peroxide ( $H_2O_2$ ) can lead to the recombination of hydroxyl radicals ( $HO^\bullet$ ) to form hydroperoxyl radicals ( $HO_2^\bullet$ ), as shown in Equation (11). Hydroperoxyl radicals have a lower oxidation potential than hydroxyl radicals, so they are less effective at degrading the target molecules. In addition, an excess of  $H_2O_2$  can accelerate its self-decomposition, producing  $O_2$  and  $H_2O$ , as shown in Equation (12), but not reactive radicals [20]. This phenomenon is known as the competition effect.



Several studies have shown that increasing the concentration of hydrogen peroxide ( $H_2O_2$ ) leads to an increase in the production of hydroxyl radicals. This is important because hydroxyl radicals are highly reactive and can degrade a wide variety of molecules, including antibiotic compounds. For example, a study on the degradation of Gatifloxacin found that increasing the  $H_2O_2$  concentration from 0.4 to 1.6 mM increased the degradation rate of Gatifloxacin to 97% [38]. Similar patterns have been shown in previous studies with other antibiotics [39–41]. These studies demonstrate that  $H_2O_2$  can be an effective way to degrade antibiotic compounds. However, it is important to note that increasing the  $H_2O_2$  concentration too much can lead to the formation of other harmful byproducts, such as hydroperoxyl radicals. Therefore, it is important to use the correct concentration of  $H_2O_2$  for the specific application.

The correlation coefficients ( $R^2$ ) and the DOX removal (%) during the solar photo-Fenton reaction are shown in Table 3. The degradation profile aligned well with pseudo-first-order kinetics, with an  $R^2$  value of 0.99 at the optimal concentration of  $H_2O_2$ . Clearly, the higher the dosage of  $H_2O_2$ , the slower the degradation of DOX. R.S. Cardenas Sierra et al. [42] discovered that increasing the  $H_2O_2$  concentration is positive for achieving a higher DOX elimination using simulated sunlight and  $H_2O_2$ . The degradation of DOX was affected by the  $H_2O_2$  starting concentration; raising the initial concentration of  $H_2O_2$  from 3 mM to 5 mM resulted in a drop in rate constants from 0.004 to 0.003  $\text{min}^{-1}$  with an optimum value of 0.013  $\text{min}^{-1}$  at 4 mM of  $H_2O_2$ .

**Table 3.** Kinetic parameters, correlation coefficients ( $R^2$ ), and % DOX removal of the DOX elimination via the solar photo-Fenton process.

$H_2O_2$ (mM)	$K$ ( $\text{min}^{-1}$ ) $\times 10^{-1}$	$R^2$	DOX Removal (%)
3	0.04	0.94	51.00
4	0.13	0.99	90.00
5	0.03	0.97	43.10

### 3.1.3. Effect of Initial DOX Concentration

The impact of initial DOX concentration on photo-Fenton treatment was studied. Several concentrations ranging from 0.02 to 0.22 mM were investigated with an  $[H_2O_2]/[Fe^{2+}]$  ratio of 40, which is close to other ratio values reported for other organic compounds [34,43]. The DOX removal rate decreases from 87.4 to 56.6% when the DOX concentration is raised from 0.02 to 0.22 mM, with an optimum DOX elimination at 0.06 mM, as shown in Figure 4. This behavior is anticipated and can be explained by increasing the number of DOX molecules created for the same number of  $^\bullet OH$  generated under the same operating conditions.

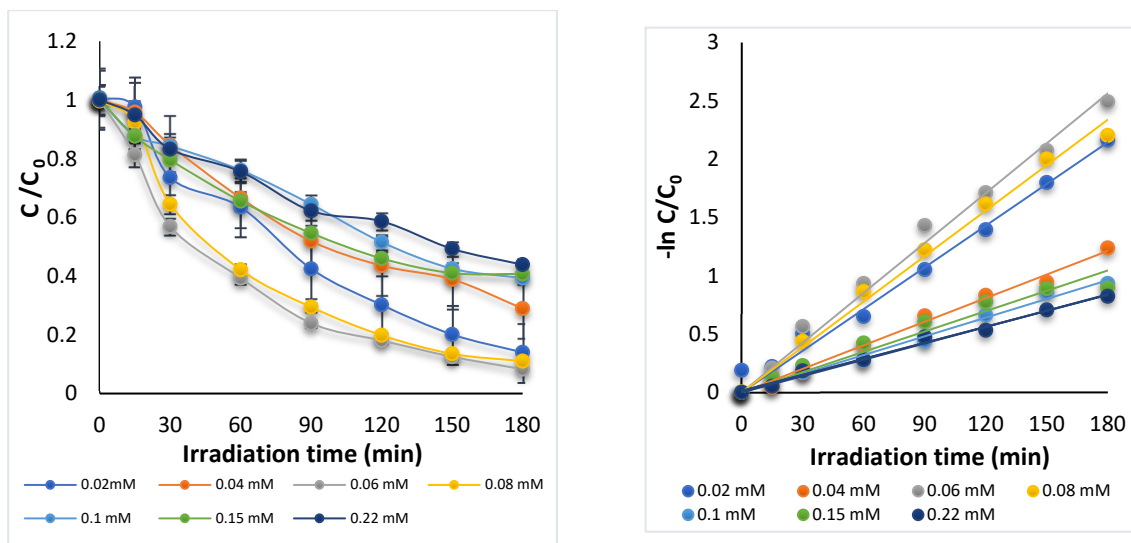


**Figure 4.** Effect of initial [DOX] on the solar photo-Fenton process at optimized conditions:  $[\text{H}_2\text{O}_2] = 4 \text{ mM}$ ,  $[\text{Fe}^{2+}] = 0.1 \text{ mM}$ ,  $\text{pH} = 3$ .

Table 4 shows that the solar photo-Fenton reaction rate of DOX removal obeyed the pseudo-first-order kinetics and that the degradation of DOX was dependent on its initial concentration; increasing DOX initial concentration from 0.02 to 0.22 mM led to the decrease of the rate constants from 0.0119 to 0.0047  $\text{min}^{-1}$  with an optimum value at 0.06 mM of DOX where the degradation achieved 91.7% with a correlation coefficient ( $R^2 = 0.99$ ).

**Table 4.** Kinetic parameters correlation coefficients ( $R^2$ ) and DOX removal (%) of the DOX elimination via the solar photo-Fenton process.

DOX (mM)	K ( $\text{min}^{-1}$ )	$R^2$	DOX Removal (%)
0.02	0.0119	0.99	87.4
0.04	0.0067	0.99	71.0
0.06	0.0142	0.99	91.7
0.08	0.0130	0.99	88.0
0.100	0.0053	0.98	60.7
0.150	0.0058	0.94	59.2
0.220	0.0047	0.99	56.1

### 3.2. Solar Photo-Fenton (SPF) at Optimum Conditions

The photochemical degradation of the DOX by the solar photo-Fenton process was studied using  $\text{Fe}^{2+}$  as a catalyst and  $\text{H}_2\text{O}_2$  as an oxidant at optimized conditions. The experiments were carried out in a CPC reactor under solar irradiation between 11 a.m. and 3 p.m. with similar weather conditions in August 2022 for 180 min.

The optical density of the DOX solution before and after the solar photo-Fenton treatment using spectrum analysis is depicted in Figure 5. The pharmaceutical molecule represents two  $\lambda_{\text{max}}$  at 278 nm and 350 nm. If the DOX molecule shares the same structural basis with tetracycline and differs in a few functional groups only, the behavior of tetracycline may be applied to DOX molecules. Therefore, we deduce that DOX absorbs in the UV-B range (250 to 300 nm) thanks to the tricarbonyl amide group on the DOX (A ring), and it absorbs in the two ranges from 250 to 300 nm (UV-B), 340–380 nm (UV-A) thanks to the phenolic diketone on the DOX (B-C-D rings) [29,44,45]. The amount of DOX removed (%) was monitored at 350 nm (the absorbance of the treated DOX solution was read at a wavelength of 350 nm),  $\text{H}_2\text{O}_2$  absorbs at UV wavelengths spanning from 300 nm



to 124 nm, with a maximum absorption at 250 nm [46]. As is widely known,  $H_2O_2$  may affect the spectrophotometric graph of DOX in the UV-B region [47].

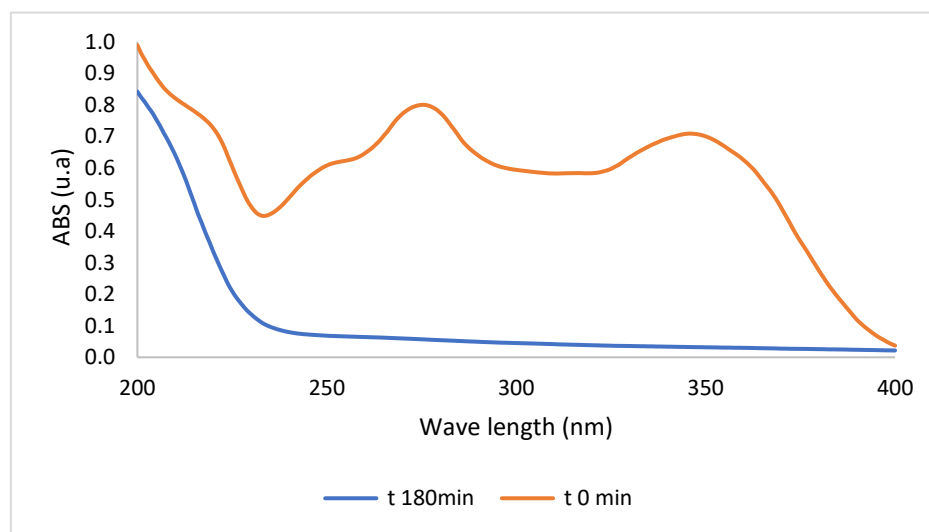
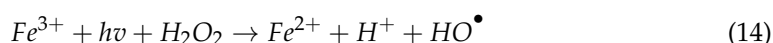


**Figure 5.** Spectral scanning of DOX solution before and after the solar photo-Fenton treatment at optimized conditions:  $[DOX] = 0.06$  mM,  $[H_2O_2] = 4$  mM,  $[Fe^{2+}] = 0.1$  mM.

The efficiency of the treatment was calculated by Equation (5) before and after the solar photo-Fenton treatment. A DOX removal yield of 95.07% at 350 nm was established by spectral scanning after an irradiation time of 180 min, which is equivalent to a DOX concentration drop from 0.06 mM to 0.0029 mM. This could be explained by the breakdown of the organic molecule by the high production of hydroxyl radicals resulting from the Fenton reaction in the first place, as shown in Equation (1), then the cleavage of  $H_2O_2$ , as shown in Equation (13), and by the reduction of  $Fe^{3+}$  with  $H_2O_2$  under a light source, as shown in Equation (14).



The medium's pH was adjusted to 3 to prevent the precipitation of dissolved iron after combining with  $OH^-$ . Adding to that the DOX state in acidic pH results in the existence of 45(%) of zwitterionic  $DOX^0$  and 55(%) of cationic  $DOX^+$  as shown in Figure 6. Thus, DOX is easily excited electronically by the illumination source [48].

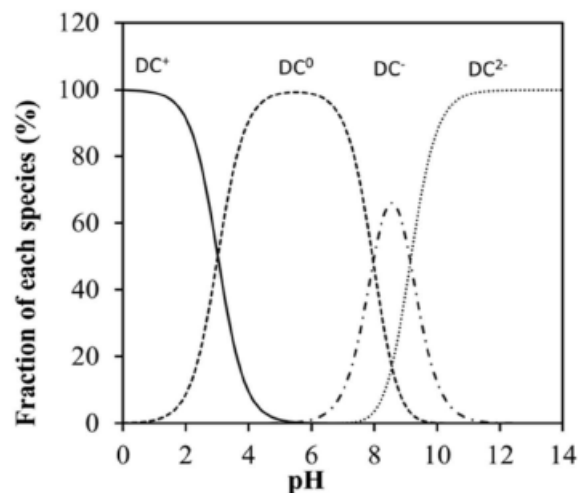


**Figure 6.** DOX speciation at different pH [48].

To corroborate the findings, an HPLC analysis before and after the SPF treatment was carried out. The DOX concentration declined from 0.06 mM to 0.0066 mM at 350 nm with a DOX removal of 88.44%, which is in agreement with the results of previous studies on antibiotics photodegradation using the same oxidation process that indicates a complete degradation rate of antibiotics [17,21,49,50]. The obtained results of the elimination of the total organic carbon and the chemical oxygen demand before and after solar photo-Fenton treatment are listed in Table 5.

**Table 5.** DOX mineralization before and after the SPF treatment.

	TOC	COD
Before treatment	17.67 ± 1.14 mg/L	53.33 ± 4.79 mg O <sub>2</sub> /L
After treatment	4.75 ± 0.04 mg/L	9.9 ± 4.63 mg O <sub>2</sub> /L
Removal rate (%)	73.05	81.43

The applied degradation process reduced the total organic carbon content from 17.67 mg/L (corresponding to 0.06 mM DOX at the initial phase of the treatment) to 4.75 mg/L, with a total organic carbon removal rate of 73.05%. As well, the results indicate a COD elimination effectiveness of 81.43% following the solar photo-Fenton treatment. The mineralization findings are significant when compared to prior research employing advanced oxidation techniques for DOX as well as antibiotics elimination. Table 6 shows the previous mineralization results using the solar photo-Fenton process on a pilot scale.

**Table 6.** Comparison of DOX mineralization with previous works using the solar photo-Fenton process on a pilot scale.

Pharmaceutical Pollutant	[H <sub>2</sub> O <sub>2</sub> ]/[Fe <sup>2+</sup> ] Ratio	Type and Time of the Process	Pollutant Removal (%)	COD Removal (%)	References
ofloxacin (OFX) and trimethoprim (TMP).	15.0	SPF 180 min	100%	21%	[51]
sulfamethoxazole (SMX) and erythromycin (ERY)	10.0	SPF 120 min	100%	53%	[41]
Ampicillin (AMP)	10.0	SPF 180 min	95%	24%	[49]
Isoniazid (INH)	12.5	SPF 120 min	99.99%	70%	[17]
Amoxicillin, Ampicillin, Diclofenac, and Paracetamol	3	SPF 120 min	100%	-	[40]
nalidixic acid	15	SPF 190 min	99.99%	33%	[52]
Tetracycline	0.67	SPF 120 min	88.7%	-	[37]
Doxycycline (DOX)	40.0	SPF 180 min	95.07%	81%	This study

In the literature, the effectiveness of DOX elimination by advanced oxidation processes does not mean a high mineralization rate. In particular, in the research on DOX removal using simulated solar radiation and H<sub>2</sub>O<sub>2</sub>, the COD was decreased by 43.0% while NO<sub>3</sub> increased significantly [42]. In the paper of Borghi et al. [53] about DOX removal using the Fenton process, the total organic carbon cannot be reduced by more than 30%. In another study by Ioannou-Ttofa et al. [49], an ampicillin removal of 99.99% was achieved after 30 min of the solar photo-Fenton process yet the efficiency of TOC removal was about 24%. The results observed in this study indicate that the SPF treatment was highly effective on DOX degradation as well as DOX mineralization.

### 3.3. Phytotoxicity Test

The phytotoxicity test was performed on two DOX samples before and after the solar photo-Fenton treatment. The germination index GI (%) was calculated with Equation (8). Based on GI percentages, compounds (and by-products) can be classified into three categories: high phytotoxicity when the GI is less than 50%, moderate phytotoxicity when  $50\% < GI < 80\%$ , and no phytotoxicity when the GI value is greater than 80% [31]. Figure 7 shows the phytotoxicity results of the DOX solution at a concentration of 0.06 mM before and after treatment. The DOX solution before treatment has moderate phytotoxicity with a germination index of 50.25%. However, after treatment by the solar photo-Fenton process of 3 h, a decrease in phytotoxicity with a germination index of 125.57% was obtained. Therefore, it can be concluded that the treatment was effective and that the DOX by-products are non-toxic to watercress seeds.

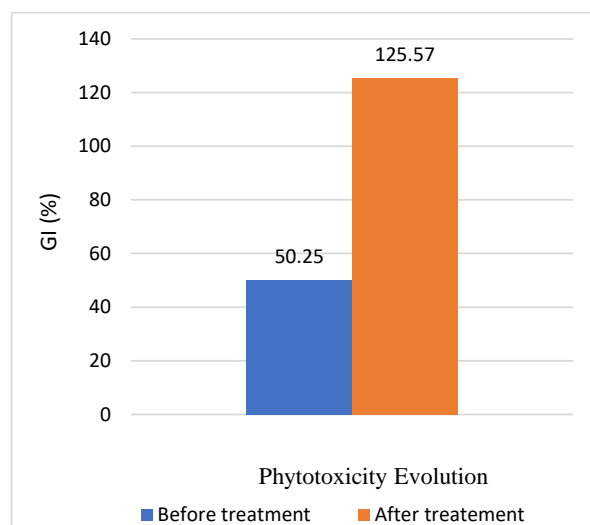


**Figure 7.** Phytotoxicity evolution before and after solar photo-Fenton treatment at optimal conditions during 180 min.

## 4. Conclusions

The degradation of DOX in a solar CPC pilot plant by the SPF process was investigated in this paper. The best initial concentrations of ferrous ions, hydrogen peroxide, and DOX were tuned to maximize DOX removal. The optimal experimental conditions for removing 95.07% of DOX were  $[Fe^{2+}] = 0.1$  mM,  $[H_2O_2] = 4$  mM, and  $[DOX] = 0.06$  mM. The TOC and COD readings fell by 73.05% and 81.43%, respectively, demonstrating that the SPF technique produced less dangerous DOX oxidation products. The phytotoxicity tests with watercress seeds had an index of germination of 125.57%, indicating that the by-products formed by the SPF treatment may be eliminated by biological treatment. As a result, combining the SPF process with biological treatment has the potential to be beneficial. The solar photo-Fenton process has been proven to be physically and operationally feasible on a pilot scale for doxycycline degradation, with both economic and environmental benefits because there is no energy consumption spent for the illumination of the CPC reactor, making it easier for treatment plants to employ this ecofriendly procedure. Peak periods of sunlight, fluctuations in daylight, and seasonal variations in amounts of direct and diffuse radiation from one region to another can impact solar process efficiency. Thus, further research is needed to optimize the SPF process for the degradation of doxycycline under different conditions.

**Author Contributions:** F.B.: Investigation, Methodology, Writing—original draft; M.C.: Supervision, Review and Editing, Funding acquisition; H.D.: Supervision, Review and Editing, Funding acquisition; S.B.: Conceptualization, Methodology, Resources. All authors have read and agreed to the published version of the manuscript.

**Funding:** The authors are grateful to the Directorate General for Scientific Research and Technological Development “DGRSDT Algeria” for financial support.

**Data Availability Statement:** Data used to support the study’s findings can be obtained from the corresponding authors upon request.

**Acknowledgments:** Clarisse Roig from Unilasalle Rennes, for her technical help.

**Conflicts of Interest:** The authors declare no conflict of interest.

## References

1. Kümmerer, K. Antibiotics in the aquatic environment—A review—Part I. *Chemosphere* **2009**, *75*, 417–434. [[CrossRef](#)] [[PubMed](#)]
2. Begum, S.; Begum, T.; Rahman, N.; Khan, R.A. A review on antibiotic resistance and way of combating antimicrobial resistance. *GSC Biol. Pharm. Sci.* **2021**, *14*, 87–97. [[CrossRef](#)]
3. Rizzo, L. Addressing main challenges in the tertiary treatment of urban wastewater: Are homogeneous photodriven AOPs the answer? *Environ. Sci. Water Res. Technol.* **2022**, *8*, 2145–2169. [[CrossRef](#)]
4. Jodh, R.; Tawar, M.; Gomkale, K.; Jari, S.; Topley, J.; Faisal, N. An Updated Review on Doxycycline. *Res. J. Pharmacol. Pharmacodyn.* **2022**, *14*, 253–256. [[CrossRef](#)]
5. Amangelsin, Y.; Semenova, Y.; Dadar, M.; Aljofan, M.; Bjørklund, G. The Impact of Tetracycline Pollution on the Aquatic Environment and Removal Strategies. *Antibiotics* **2023**, *12*, 440. [[CrossRef](#)]
6. Nam, S.W.; Jo, B.I.; Yoon, Y.; Zoh, K.D. Occurrence and removal of selected micropollutants in a water treatment plant. *Chemosphere* **2014**, *95*, 156–165. [[CrossRef](#)]
7. Yanovych, D.; Zasadna, Z.; Rydchuk, M.; Plotycya, S.; Kislova, S.; Pazderska, O.; Ivach, S. Doxycycline dertermination in animal tissues and blood plasma samples using screening and confirmatory methods. *Sci. Tech. Bull. State Sci. Res. Control Inst. Vet. Med. Prod. Fodd. Addit. Inst. Anim. Biol.* **2021**, *22*, 432–446. [[CrossRef](#)]
8. Yan, Q.; Li, X.; Ma, B.; Zou, Y.; Wang, Y.; Liao, X.; Liang, J.; Mi, J.; Wu, Y. Different Concentrations of Doxycycline in Swine Manure Affect the Microbiome and Degradation of Doxycycline Residue in Soil. *Front. Microbiol.* **2018**, *9*, 3129. [[CrossRef](#)]
9. Deng, W.; Li, N.; Zheng, H.; Lin, H. Occurrence and risk assessment of antibiotics in river water in Hong Kong. *Ecotoxicol. Environ. Saf.* **2016**, *125*, 121–127. [[CrossRef](#)]
10. Bu, Q.; Wang, B.; Huang, J.; Deng, S.; Yu, G. Pharmaceuticals and personal care products in the aquatic environment in China: A review. *J. Hazard. Mater.* **2013**, *262*, 189–211. [[CrossRef](#)]
11. Kanama, K.M.; Daso, A.P.; Mpenyana-Monyatsi, L.; Coetzee, M.A.A. Assessment of Pharmaceuticals, Personal Care Products, and Hormones in Wastewater Treatment Plants Receiving Inflows from Health Facilities in North West Province, South Africa. *J. Toxicol.* **2018**, *2018*, 3751930. [[CrossRef](#)]
12. Aga, D.S.; O’Connor, S.; Ensley, S.; Payero, J.O.; Snow, D.; Tarkalson, D. Determination of the persistence of tetracycline antibiotics and their degradates in manure-amended soil using enzyme-linked immunosorbent assay and liquid chromatography-mass spectrometry. *J. Agric. Food Chem.* **2005**, *53*, 7165–7171. [[CrossRef](#)] [[PubMed](#)]
13. Jiang, Y.; Ran, J.; Mao, K.; Yang, X.; Zhong, L.; Yang, C.; Feng, X.; Zhang, H. Recent progress in Fenton/Fenton-like reactions for the removal of antibiotics in aqueous environments. *Ecotoxicol. Environ. Saf.* **2022**, *236*, 113464. [[CrossRef](#)] [[PubMed](#)]
14. Park, J.A.; Pineda, M.; Peyot, M.L.; Yargeau, V. Degradation of oxytetracycline and doxycycline by ozonation: Degradation pathways and toxicity assessment. *Sci. Total Environ.* **2023**, *856*, 159076. [[CrossRef](#)] [[PubMed](#)]
15. Yu, R.; Ma, R.; Wang, L.; Bai, L.; Yang, S.; Qian, J. Activation of peroxydisulfate (PDS) by Bi<sub>5</sub>O<sub>7</sub>I@MIL-100(Fe) for catalytic degradation of aqueous doxycycline (DOX) under UV light irradiation: Characteristic, performance and mechanism. *J. Water Process Eng.* **2022**, *48*, 102903. [[CrossRef](#)]
16. Aboudalle, A.; Djelal, H.; Domergue, L.; Fourcade, F.; Amrane, A. A novel system coupling an electro-Fenton process and an advanced biological process to remove a pharmaceutical compound, metronidazole. *J. Hazard. Mater.* **2021**, *415*, 125705. [[CrossRef](#)]
17. Rodrigues-Silva, F.; Lemos, C.R.; Naico, A.A.; Fachi, M.M.; do Amaral, B.; de Paula, V.C.S.; Rampon, D.S.; Beraldi-Magalhães, F.; Prola, L.D.T.; Pontarolo, R.; et al. Study of isoniazid degradation by Fenton and photo-Fenton processes, by-products analysis and toxicity evaluation. *J. Photochem. Photobiol. A Chem.* **2022**, *425*, 113671. [[CrossRef](#)]
18. Babuponnusami, A.; Muthukumar, K. A review on Fenton and improvements to the Fenton process for wastewater treatment. *J. Environ. Chem. Eng.* **2014**, *2*, 557–572. [[CrossRef](#)]
19. Phoon, B.L.; Ong, C.C.; Mohamed Saheed, M.S.; Show, P.L.; Chang, J.S.; Ling, T.C.; Lam, S.S.; Juan, J.C. Conventional and emerging technologies for removal of antibiotics from wastewater. *J. Hazard. Mater.* **2020**, *400*, 122961. [[CrossRef](#)]
20. Pignatello, J.J.; Oliveros, E.; MacKay, A. Advanced Oxidation Processes for Organic Contaminant Destruction Based on the Fenton Reaction and Related Chemistry. *Crit. Rev. Environ. Sci. Technol.* **2007**, *36*, 1–84. [[CrossRef](#)]
21. Han, C.; Park, H.; Kim, S.; Yargeau, V.; Choi, J.; Lee, S.; Park, J. Oxidation of tetracycline and oxytetracycline for the photo-Fenton process: Their transformation products and toxicity assessment. *Water Res.* **2020**, *172*, 115514. [[CrossRef](#)] [[PubMed](#)]

22. Zhong, J.; Yang, B.; Gao, F.Z.; Xiong, Q.; Feng, Y.; Li, Y.; Zhang, J.N.; Ying, G.G. Performance and mechanism in degradation of typical antibiotics and antibiotic resistance genes by magnetic resin-mediated UV-Fenton process. *Ecotoxicol. Environ. Saf.* **2021**, *227*, 112908. [[CrossRef](#)] [[PubMed](#)]
23. Belalcázar-Saldarriaga, A.; Prato-Garcia, D.; Vasquez-Medrano, R. Photo-Fenton processes in raceway reactors: Technical, economic, and environmental implications during treatment of colored wastewaters. *J. Clean. Prod.* **2018**, *182*, 818–829. [[CrossRef](#)]
24. Periša, M.; Babić, S.; Škorić, I.; Frömel, T.; Knepper, T.P. Photodegradation of sulfonamides and their N (4)-acetylated metabolites in water by simulated sunlight irradiation: Kinetics and identification of photoproducts. *Environ. Sci. Pollut. Res. Int.* **2013**, *20*, 8934–8946. [[CrossRef](#)] [[PubMed](#)]
25. Muñoz, I.; Rieradevall, J.; Torrades, F.; Peral, J.; Domènech, X. Environmental assessment of different solar driven advanced oxidation processes. *Sol. Energy* **2005**, *79*, 369–375. [[CrossRef](#)]
26. Rocha, E.M.R.; Vilar, V.J.P.; Fonseca, A.; Saraiva, I.; Boaventura, R.A.R. Landfill leachate treatment by solar-driven AOPs. *Sol. Energy* **2011**, *85*, 46–56. [[CrossRef](#)]
27. Nascimento, C.A.O.; Teixeira, A.C.S.C.; Guardani, R.; Quina, F.H.; Chiavone-Filho, O.; Braun, A.M. Industrial wastewater treatment by photochemical processes based on solar energy. *J. Sol. Energy Eng. Trans. ASME* **2007**, *129*, 45–52. [[CrossRef](#)]
28. Malato, S.; Fernández-Ibáñez, P.; Maldonado, M.I.; Blanco, J.; Gernjak, W. Decontamination and disinfection of water by solar photocatalysis: Recent overview and trends. *Catal. Today* **2009**, *147*, 1–59. [[CrossRef](#)]
29. Bolobajev, J.; Trapido, M.; Goi, A. Effect of iron ion on doxycycline photocatalytic and Fenton-based autocatalytic decomposition. *Chemosphere* **2016**, *153*, 220–226. [[CrossRef](#)]
30. Sunarić, S.M.; Denić, M.S.; Bojanić, Z.Ž.; Bojanić, V.V. HPLC method development for determination of doxycycline in human seminal fluid. *J. Chromatogr. B* **2013**, *939*, 17–22. [[CrossRef](#)]
31. Zeghioud, H.; Khellaf, N.; Amrane, A.; Djelal, H.; Bouhelassa, M.; Assadi, A.A.; Rtimi, S. Combining photocatalytic process and biological treatment for Reactive Green 12 degradation: Optimization, mineralization, and phytotoxicity with seed germination. *Environ. Sci. Pollut. Res.* **2021**, *28*, 12490–12499. [[CrossRef](#)] [[PubMed](#)]
32. Cherif, S.; Djelal, H.; Firmin, S.; Bonnet, P.; Frezet, L.; Kane, A.; Amine Assadi, A.; Trari, M.; Yazid, H. The impact of material design on the photocatalytic removal efficiency and toxicity of two textile dyes. *Environ. Sci. Pollut. Res.* **2022**, *29*, 66640–66658. [[CrossRef](#)] [[PubMed](#)]
33. Rahim Pouran, S.; Abdul Aziz, A.R.; Wan Daud, W.M.A. Review on the main advances in photo-Fenton oxidation system for recalcitrant wastewaters. *J. Ind. Eng. Chem.* **2015**, *21*, 53–69. [[CrossRef](#)]
34. Zhang, Y.; Pagilla, K. Treatment of malathion pesticide wastewater with nanofiltration and photo-Fenton oxidation. *Desalination* **2010**, *263*, 36–44. [[CrossRef](#)]
35. Lucas, M.S.; Peres, J.A. Decolorization of the azo dye Reactive Black 5 by Fenton and photo-Fenton oxidation. *Dye. Pigment.* **2006**, *71*, 236–244. [[CrossRef](#)]
36. Loaiza-Ambuludi, S.; Panizza, M.; Oturan, N.; Oturan, M.A. Removal of the anti-inflammatory drug ibuprofen from water using homogeneous photocatalysis. *Catal. Today* **2014**, *224*, 29–33. [[CrossRef](#)]
37. Cahino, A.M.; de Andrade, M.M.A.; de Araújo, E.S.; Silva, E.L.; Cunha, C.D.O.; Rocha, E.M.R. Degradation of tetracycline by solar photo-Fenton: Optimization and application in pilot photoreactor. *Environ. Qual. Manag.* **2018**, *28*, 101–106. [[CrossRef](#)]
38. Caianelo, M.; Rodrigues-Silva, C.; Maniero, M.G.; Guimarães, J.R. Antimicrobial activity against Gram-positive and Gram-negative bacteria during gatifloxacin degradation by hydroxyl radicals. *Environ. Sci. Pollut. Res.* **2017**, *24*, 6288–6298. [[CrossRef](#)]
39. Giannakis, S.; Gamarra Vives, F.A.; Grandjean, D.; Magnet, A.; De Alencastro, L.F.; Pulgarin, C. Effect of advanced oxidation processes on the micropollutants and the effluent organic matter contained in municipal wastewater previously treated by three different secondary methods. *Water Res.* **2015**, *84*, 295–306. [[CrossRef](#)]
40. Alalm, M.G.; Tawfik, A.; Ookawara, S. Degradation of four pharmaceuticals by solar photo-Fenton process: Kinetics and costs estimation. *J. Environ. Chem. Eng.* **2015**, *3*, 46–51. [[CrossRef](#)]
41. Karaolia, P.; Michael-Kordatou, I.; Hapeshi, E.; Alexander, J.; Schwartz, T.; Fatta-Kassinos, D. Investigation of the potential of a Membrane BioReactor followed by solar Fenton oxidation to remove antibiotic-related microcontaminants. *Chem. Eng. J.* **2017**, *310*, 491–502. [[CrossRef](#)]
42. Cárdenas Sierra, R.S.; Zúñiga-Benítez, H.; Peñuela, G.A. Photo-assisted removal of doxycycline using H<sub>2</sub>O<sub>2</sub> and simulated sunlight: Operational parameters optimization and ecotoxicity assessment. *J. Photochem. Photobiol. A Chem.* **2022**, *425*. [[CrossRef](#)]
43. Annabi, C.; Abou Dalle, A.; Fourcade, F.; Assadi, A.A.; Soutrel, I.; Bellakhal, N.; Amrane, A. Enoxacin degradation by photo-Fenton process combined with a biological treatment: Optimization and improvement of by-products biodegradability. *Int. J. Environ. Sci. Technol.* **2019**, *16*, 655–666. [[CrossRef](#)]
44. Li, S.; He, Y.; Kong, F.; Sun, W.; Hu, J. Photolytic Degradation of Tetracycline in the Presence of Ca(II) and/or Humic Acid. *Water* **2020**, *12*, 2078. [[CrossRef](#)]
45. Chen, W.R.; Huang, C.H. Transformation of tetracyclines mediated by Mn(II) and Cu(II) ions in the presence of oxygen. *Environ. Sci. Technol.* **2009**, *43*, 401–407. [[CrossRef](#)] [[PubMed](#)]
46. Aye, T.T.; Low, T.Y.; Sze, S.K. Nanosecond laser-induced photochemical oxidation method for protein surface mapping with mass spectrometry. *Anal. Chem.* **2005**, *77*, 5814–5822. [[CrossRef](#)]

47. Mota, A.L.N.; Muranaka, C.T.; Moraes, J.E.F.; Nascimento, C.A.O. *Aplicação do Processo Foto-Fenton na Fotodegradação do Fenol em Meio Aquoso Utilizando l'Ampadas de Luz Negra como Fonte de Radiação*; Federation de Ingenieros Quimicos del Peru: Peru, Lima, 2005.
48. Álvarez-Esmoris, C.; Rodríguez-López, L.; Fernández-Calviño, D.; Núñez-Delgado, A.; Álvarez-Rodríguez, E.; Arias-Estévez, M. Degradation of Doxycycline, Enrofloxacin, and Sulfamethoxypyridazine under Simulated Sunlight at Different pH Values and Chemical Environments. *Agronomy* **2022**, *12*, 260. [[CrossRef](#)]
49. Ioannou-Ttofa, L.; Raj, S.; Prakash, H.; Fatta-Kassinos, D. Solar photo-Fenton oxidation for the removal of ampicillin, total cultivable and resistant *E. coli* and ecotoxicity from secondary-treated wastewater effluents. *Chem. Eng. J.* **2019**, *355*, 91–102. [[CrossRef](#)]
50. da Costa, E.P.; Bottrel, S.E.C.; Starling, M.C.V.M.; Leão, M.M.D.; Amorim, C.C. Degradation of carbendazim in water via photo-Fenton in Raceway Pond Reactor: Assessment of acute toxicity and transformation products. *Environ. Sci. Pollut. Res.* **2019**, *26*, 4324–4336. [[CrossRef](#)]
51. Michael, I.; Hapeshi, E.; Michael, C.; Varela, A.R.; Kyriakou, S.; Manaia, C.M.; Fatta-Kassinos, D. Solar photo-Fenton process on the abatement of antibiotics at a pilot scale: Degradation kinetics, ecotoxicity and phytotoxicity assessment and removal of antibiotic resistant enterococci. *Water Res.* **2012**, *46*, 5621–5634. [[CrossRef](#)]
52. Sirtori, C.; Zapata, A.; Oller, I.; Gernjak, W.; Agüera, A.; Malato, S. Decontamination industrial pharmaceutical wastewater by combining solar photo-Fenton and biological treatment. *Water Res.* **2009**, *43*, 661–668. [[CrossRef](#)] [[PubMed](#)]
53. Borghi, A.A.; Silva, M.F.; Al Arni, S.; Converti, A.; Palma, M.S.A. Doxycycline degradation by the oxidative Fenton process. *J. Chem.* **2015**, *2015*, 492030. [[CrossRef](#)]

**Disclaimer/Publisher's Note:** The statements, opinions and data contained in all publications are solely those of the individual author(s) and contributor(s) and not of MDPI and/or the editor(s). MDPI and/or the editor(s) disclaim responsibility for any injury to people or property resulting from any ideas, methods, instructions or products referred to in the content.